Tree Physiology 36, 1562–1572
doi:10.1093/treephys/tpw073

Research paper

Osmotic and hydraulic adjustment of mangrove saplings to extreme salinity

Rodrigo Méndez-Alonzo[1,5], Jorge López-Portillo[2], Coral Moctezuma[3], Megan K. Bartlett[4] and Lawren Sack[4]

[1]Departamento de Biología de la Conservación, Centro de Investigación Científica y de Educación Superior de Ensenada (CICESE), Carretera Ensenada-Tijuana No. 3918, Zona Playitas, Ensenada, B.C., 22860, México; [2]Red de Ecología Funcional, Instituto de Ecología, A.C., Xalapa, Veracruz, 91070, México; [3]Instituto de Investigaciones en Ecosistemas y Sustentabilidad, Universidad Nacional Autónoma de México, Morelia, Michoacán, 58190 , México; [4]Department of Ecology and Evolutionary Biology, University of California Los Angeles, Los Angeles, CA 90095-1606, USA; [5]Corresponding author (mendezal@cicese.mx)

Received December 17, 2015; accepted July 12, 2016; published online September 2, 2016; handling Editor Marilyn Ball

Salinity tolerance in plant species varies widely due to adaptation and acclimation processes at the cellular and whole-plant scales. In mangroves, extreme substrate salinity induces hydraulic failure and ion excess toxicity and reduces growth and survival, thus suggesting a potentially critical role for physiological acclimation to salinity. We tested the hypothesis that osmotic adjustment, a key type of plasticity that mitigates salinity shock, would take place in coordination with declines in whole-plant hydraulic conductance in a common garden experiment using saplings of three mangrove species with different salinity tolerances (*Avicennia germinans* L., *Rhizophora mangle* L. and *Laguncularia racemosa* (L.) C.F. Gaertn., ordered from higher to lower salinity tolerance). For each mangrove species, four salinity treatments (1, 10, 30 and 50 practical salinity units) were established and the time trajectories were determined for leaf osmotic potential (Ψ_s), stomatal conductance (g_s), whole-plant hydraulic conductance (K_{plant}) and predawn disequilibrium between xylem and substrate water potentials (Ψ_{pdd}). We expected that, for all three species, salinity increments would result in coordinated declines in Ψ_s, g_s and K_{plant}, and that the Ψ_{pdd} would increase with substrate salinity and time of exposure. In concordance with our predictions, reductions in substrate water potential promoted a coordinated decline in Ψ_s, g_s and K_{plant}, whereas the Ψ_{pdd} increased substantially during the first 4 days but dissipated after 7 days, indicating a time lag for equilibration after a change in substratum salinity. Our results show that mangroves confront and partially ameliorate acute salinity stress via simultaneous reductions in Ψ_s, g_s and K_{plant}, thus developing synergistic physiological responses at the cell and whole-plant scales.

Keywords: mangroves, Mexico, plant turgor, predawn disequilibrium, salinity stress, saplings, stomatal conductance.

Introduction

Adaptation to water-logging and substrate salinity occurs in multiple lineages of mangrove arboreal species (Ball 1988, Shi et al. 2005, Moray et al. 2015). Besides inundation frequency, salinity is probably the most important environmental factor that drives the local distribution of mangrove species (Lugo and Snedaker 1974). In mangroves there is a spectrum of salinity tolerance across species, ranging from functional halophytes, which achieve their maximum growth at salinities from 5 to 25 practical salinity units (PSU) (Burchett et al. 1984, Ball 2002, Patel et al. 2010, Nguyen et al. 2015), to facultative halophytes and glycophytes, which achieve their maximum growth in fresh water (Wang et al. 2011, Krauss and Ball 2013, Lovelock et al. 2016). The genus *Avicennia* includes some of the most salinity-tolerant species (López-Hoffmann et al. 2006, 2007). In particular, *Avicennia marina* (Forsk.) Vierh., one of the most salt-tolerant mangrove species, can resist and recover from salinity shocks under experimental conditions; when exposed to salinities

~35 PSU the photosynthetic rate and stomatal conductance were reduced, but when re-exposed to a salinity of 3.5 PSU it could nearly recover its gas exchange functions (Ball and Farquhar 1984*a*). When less salinity-tolerant species, such as *Rhizophora mangle* L., are exposed to high salinity substrates, a strong reduction in carbon assimilation and growth rate occur, along with an increase in the respiration rate; however, whether this species is able to recover its growth rate and gas exchange functions if re-exposed to lower salinity levels has not been determined (Krauss and Allen, 2003, López-Hoffman et al. 2006, 2007).

This variation in the salinity growth-optimum range across mangroves is associated with physiological responses at the cell, organ and whole-plant scales. Mangroves have mechanisms to exclude, secrete and accumulate ions, such as the ultrafiltration of salt in the roots, salt glands, hyper-accumulation of ions in the vacuoles and the production of compatible solutes (Scholander 1968, Parida and Jha 2010, Reef and Lovelock 2015). However, when salinity is higher than seawater, mangroves respond with more frequent events of stomatal closure, which not only reduces net rates of photosynthesis and growth (Burchett et al. 1984, Ball and Farquhar 1984*a*, 1984*b*, Naidoo 1987, Suárez and Medina 2005, 2006, Yan et al. 2007), but also is associated with a decline in the whole-plant hydraulic conductance due to cavitation of the xylem, swelling or shrinkage of hydrogels in the pit membranes, selective blocking of ions due to apoplastic barriers and biseriate exodermis and/or to reductions in aquaporin abundance and activity in leaves and roots (Melcher et al. 2001, Ewers et al. 2004, López-Portillo et al. 2005, Robert et al. 2009, Tan et al. 2013, Krishnamurthy et al. 2014). To maintain plant turgor and endure the negative effects of these responses, halophytes increase the osmotic concentration in their leaves and may ameliorate further reductions in plant water potential by actively exchanging ions between the symplast and apoplast (Suárez et al.1998, Suárez and Sobrado 2000, Melcher et al. 2001, James et al. 2006, Lovelock et al. 2006, Zhu et al. 2011, 2012, López-Portillo et al. 2014). Osmotic adjustment may not be instantaneous and any ionic excess within the symplast may produce disequilibria between the substrate and the predawn leaf and stem water potentials, which can also occur even in homogeneous substrates close to field capacity (Donovan et al. 2001, 2003). Despite the importance of these mechanisms for halophyte physiology, the time trajectories of the leaf osmotic adjustment and its relation to whole-plant hydraulic conductance and substrate and predawn water potential disequilibrium have remained unknown. Given the wide variability in substrate salinity experienced by mangroves, we hypothesized that their foliar osmotic adjustment and stomatal closure may operate in a coordinated fashion to modulate xylem tensions and whole-plant hydraulic conductance, thus enabling species to acclimate across a wide range of substrate ionic concentrations. To the best of our knowledge, the role of substrate water potentials in controlling critical hydraulic and osmotic traits has not been explored.

To understand the physiological responses of mangroves to salinity gradients, we analyzed the coordinated cell and whole-plant responses to salinity stress by studying the timing of osmotic adjustment, stomatal conductance (g_s) and the plant-substratum water potential disequilibrium following a sudden increase in substrate salinity. In a common garden experiment focusing on saplings of three neotropical mangrove species with different salinity tolerance, we tested if: (i) declines in substrate water potential (Ψ_{sub}) drive an increase in leaf osmotic concentration and, thus, a decline in leaf osmotic potential (Ψ_s) to enable the maintenance of leaf turgor; (ii) if salinity reduces g_s and the whole-plant hydraulic conductance (K_{plant}) in a coordinated fashion, with the increase in leaf osmotic concentration caused by leaf dehydration and active osmotic adjustment (such that K_{plant} would be positively correlated with Ψ_s); and (iii) if the regulation of K_{plant} and Ψ_s gradually modify the acclimation of the predawn and midday leaf water potentials (Ψ_{pd} and Ψ_{md}, respectively) to a changing substrate water potential (Ψ_{sub}), leading to changes in the degree of predawn disequilibrium (Ψ_{pdd}; i.e., $\Psi_{pd} - \Psi_{sub} \neq 0$ MPa; Donovan et al. 1999). This study provides key insights into the integrated eco-physiological responses of mangroves to salinity shock.

Materials and methods

Study site and experimental design

Experiments were conducted in a common garden at the Centro de Investigaciones Costeras La Mancha, Veracruz, México (19° 33′27″N, 96° 23′04″W, 1200 mm annual precipitation, 25 °C mean annual temperature) from March to April 2013. Three dominant mangrove species from the area were studied: *Avicennia germinans* L. (Avicenniaceae), *Laguncularia racemosa* (L.) C.F. Gaertn. (Combretaceae) and *R. mangle* L. (Rhizophoraceae). Among these species, *A. germinans* is the most salt tolerant, followed by *R. mangle* and *L. racemosa*, as shown by physiological and anatomical evidence. For example, the stem water potential at 50% loss of stem xylem hydraulic conductivity is −5.7, −6.5 to 4.5 and −3.4 MPa for *Avicennia*, *Rhizophora* and *Laguncularia*, respectively (López-Portillo, unpublished data, Melcher et al. 2001, Ewers et al. 2004).

Two-year-old mangrove saplings were used for this experiment. Propagules having at least two well-developed leaves were collected in La Mancha Lagoon, transported to the field station and transplanted into monospecific growing beds (80 × 120 × 10 cm depth) located in an understory of surrounding trees in the Centro de Investigaciones Costeras La Mancha during March 2011. Light levels at the experiment site ranged between 10 and ~1100 mmol m^{-2} s^{-1}, depending on the time of day (Figure S1 available as Supplementary Data at *Tree Physiology* Online). Each bed was divided into a grid of 10 × 10 cm^2 (made with fishing line), where propagules were placed separately.

Table 1. Experimental salinity treatments to determine the variation in 14 physiological and functional traits in three species of mangroves. Salinity was quantified using an electronic salinity meter (Ultrameter II, Myron) and also by vapor pressure osmometry (VAPRO 5520, Wescor Inc.). For the equations to convert from PSU to mmol kg^{-1} to MPa, refer to Figure S1 available as Supplementary Data at *Tree Physiology* Online. Ionic composition for the commercial salt employed: Na = 11.85 g l^{-1}, K = 25.16 mg l^{-1}, Ca = 9.75 mg l^{-1}, Mg = 30.60 mg l^{-1}, chlorides = 20.84 g l^{-1}, sulfates = 140.08 mg l^{-1}, carbonates = 30 mg l^{-1} and alkalinity = 0.0005 Eq l^{-1}.

Species	Treatment (PSU)	Actual salinity (PSU ± SE)	Actual osmolarity (mmol kg^{-1} ± SE)
Avicennia germinans	1	0.7 ± 0.1	35 ± 4
	10	14.3 ± 0.5	481 ± 16
	30	36.6 ± 4.4	1212 ± 144
	50	43.3 ± 3.1	1431 ± 103
Laguncularia racemosa	1	0.9 ± 0.2	43 ± 6
	10	14.3 ± 0.4	481 ± 14
	30	34.2 ± 0.9	1134 ± 28
	50	51.0 ± 0.3	1686 ± 9
Rhizophora mangle	1	0.7 ± 0.1	36 ± 4
	10	10.5 ± 0.6	358 ± 19
	30	31.1 ± 0.8	1032 ± 26
	50	48.7 ± 0.9	1609 ± 28

Mangrove propagules were grown in fresh water without adding soil (each plant was in a 10 × 10 cm plastic bag with its original substrate). In March 2013, three saplings per growing bed with at least eight fully expanded leaves were randomly selected for the experiment. The mean sapling height and stem diameter (±SE) were 97 ± 4.3 and 1.4 ± 0.84 cm, respectively. For each mangrove species, four salinity treatments (i.e., four growing beds with three plants each) were established by adding diluted commercial sea salt (La Fina, Veracruz, México): 1 PSU corresponding to 38 ± 4.2 mM, 10 PSU (440 ± 24.9 mM), 30 PSU (1126 ± 79.2 mM) and 50 PSU (1575 ± 65.6 mM; Table 1). As the chemical composition of commercial salt may differ in the content of ions from standard seawater (Pilsen 1998), we analyzed the ionic composition of La Fina commercial salt using potentiometry for alkalinity, volumetric analyses for Ca^{+2}, Mg^{+2}, Cl^- and HCO_3, and gravimetric analyses for SO_4 (Table 1). On the first day of the experiment (Day 0), the volume of water in each growing bed was calculated and then diluted sea salt was added to achieve the desired level of salinity, as measured with a salinity meter (Ultrameter II, Myron, Carlsbad CA, USA). The salinity in each treatment was adjusted every afternoon to the target level. Quantification of 15 physiological and functional traits (Table 2) were made on four consecutive dates: Day 0 (prior to the addition of salt), and 2, 4 and 8 days after salt addition. An extra measurement date was performed for osmotic potential 33 days after salt addition.

Stomatal conductance and transpiration rate

On each of the measurement dates, between 09:00 and 11:00 h, g_s was measured for upper and lower leaf surfaces using a steady-state porometer (SC-1 Decagon Devices, Pullman, WA, USA), given that within these hours, these species reach their maximum g_s at this site (J. López-Portillo and F.W. Ewers, unpublished data). Relative humidity (RH) and air temperature were measured 1 cm below the studied leaves using a portable digital thermo-hygrometer (Pen-type hygrometer, Alaron Instruments, Newmarket, ON, Canada) at the same time as g_s measurements. The vapor pressure deficit (VPD) was calculated as VPD = $(1 - (RH \times VP_{sat}))/101.3$ kPa, where VP_{sat} is the saturation vapor pressure calculated from the Arden-Buck equation (Buck 1981, Guyot et al. 2012).

Table 2. Physiological and functional traits quantified in this study.

Trait	Abbreviation	Units
Substrate water salinity	–	PSU
Stomatal conductance	g_s	mmol m^{-2}s^{-1}
Transpiration	E	mmol m^{-2} s^{-1}
Whole-plant hydraulic conductance	K_{plant}	mmol m^{-2} s^{-1} MPa^{-1}
Substrate water potential	Ψ_{sub}	MPa
Leaf predawn water potential	Ψ_{pd}	MPa
Leaf midday water potential	Ψ_{md}	MPa
Predawn disequilibrium	Ψ_{pdd}	MPa
Leaf osmotic potential	Ψ_s	MPa
Leaf area	LA	cm^2
Leaf thickness	LT	cm
Leaf mass per area	LMA	g cm^{-2}
Leaf density	ρ_{leaf}	g cm^{-3}
Leaf dry matter content	LDMC	%
Leaf water content	LWC	%

Substrate, predawn and midday xylem water potentials

To quantify the substrate water potential (Ψ_{sub}), water adjacent to the roots was extracted using a 60-ml syringe and filter paper disks were saturated with ~0.01 ml of the extracted water to measure osmolality in a vapor pressure osmometer (VAPRO 5520, Wescor Inc., Logan, UT, USA). The values of osmolality were converted to units of water potential using calibration curves, such that 1 MPa of water potential = 375 mmol NaCl/kg water = 11.9 PSU NaCl (Figure S1 available as Supplementary Data at *Tree Physiology* Online).

On the night before each measurement date, one leaf per individual was placed within a sealable plastic bag (Whirl-Pak, Nasco, Fort Atkinson, WI, USA) with wet paper to minimize transpiration. The following morning, before sunrise (between 05:00 and 07:00 h), the leaves were cut and immediately placed in opaque plastic bags with wet towels and refrigerated. Predawn leaf water potential (Ψ_{pd}) was measured on the same day using a pressure chamber (Model 1000, PMS Instruments, Corvallis, OR, USA). Midday leaf water potential (Ψ_{md}) was determined for the same leaves measured for g_s. After measuring g_s, leaves were sealed for ~30 min in plastic bags with wet paper (Whirl-Pak, Nasco), excised and placed in opaque plastic bags and refrigerated to measure Ψ_{md} the same day. Predawn disequilibrium (Ψ_{pdd}) was calculated as $\Psi_{pd} - \Psi_{sub}$ (Ourcival and Berger 1995, Donovan et al. 1999, James et al. 2006), and the whole-plant hydraulic conductance, K_{plant} (mmol m^{-2} s^{-1} MPa^{-1}), was calculated as $K_{plant} = E/(\Psi_{pd} - \Psi_{md})$ (Nardini and Salleo 2000), where E is the transpiration rate (mmol m^{-2} s^{-1}), calculated as the product of g_s and VPD, assuming the boundary layer conductance (g_b) $\gg g_s$, given moderate wind speeds at our study site.

Leaf osmotic potential at predawn

Leaf osmotic potential (Ψ_s) was measured using an osmometer (VAPRO 5520, Wescor Inc.) for the same set of leaves used to quantify Ψ_{pd}. Ψ_s was determined using the methods described by Bartlett et al. (2012). Briefly, a 7-mm-diameter disk was cut with a hole-puncher between the major veins of each leaf. Disks were immediately wrapped in aluminum foil and frozen in liquid N_2 for at least 2 min. After freezing, the disks were punctured at least 10 times, inserted in the osmometer and measured using the auto-repeat mode, until readings were stable (<5 mmol kg^{-1}). Ψ_s was measured on the day before salinity addition (Day 0) and on four subsequent dates (Days 2, 4, 8 and 33).

Leaf morphological traits

Leaf area (LA), leaf thickness (LT), leaf mass per area (LMA), leaf density (ρ_{leaf}), leaf dry matter content (LDMC) and leaf water content (LWC) were quantified on the same set of leaves used to calculate Ψ_s and Ψ_{pd}. Leaf area (cm^2) was calculated from digital images using ImageJ (http://imagej.nih.gov/ij/), LT was determined with digital calipers (0.01 mm precision), LMA (g cm^{-2}) was calculated as leaf mass divided by LA, ρ_{leaf} as LMA divided by LT, LDMC as dry mass/fresh mass and LWC as ([100 × (1− LDMC)]) (Pérez-Harguindeguy et al. 2013). LDMC and LWC were calculated on Day 33, whereas other traits were calculated for all dates.

Statistical analyses

Due to the low number of replicates and to the lack of fit to the normal distribution for most variables, differences among treatments in LMA, ρ_{leaf}, g_s, transpiration rate, Ψ_{pdd} and Ψ_s were evaluated using the inverse of Bayes factors (BF, a value of BF >1 implies that data are *n* times better supported by the alternative hypothesis than by the null hypothesis; Jarosz and Wiley 2014) for two-way Analyses of variance (ANOVA) for each species, with salinity and measurement date as factors, and for LWC, Ψ_{pd} and Ψ_{md} using BF for one-way ANOVA, with salinity as factor. In addition, the magnitudes of Ψ_{pd} and Ψ_{md} were compared using BF *t*-tests for all individuals within each species, using the package BayesFactor (Morey et al. 2015, http://bayesfactorpcl.r-forge.r-project.org/) in R 3.2.4 (R Development Core Team 2016). The relationships between K_{plant} and Ψ_s, and between g_s and Ψ_{sub}, were assessed using Pearson correlations with K_{plant} and Ψ_s data ln-transformed, in JMP 8.0 (SAS Institute Inc., Cary, NC, USA) and Sigma Plot 10.0 (Systat Software, Inc., San Jose, CA, USA).

Results

For all three species, there were coordinated responses to extreme salinity, as Ψ_{sub}, Ψ_{pd}, Ψ_{md}, Ψ_s, g_s and K_{plant} were significantly associated (Table S1, Table S2). The sudden change in salinity and the associated decrease in Ψ_{sub} caused changes in leaf appearance, color and turgor (Figure 1). In *L. racemosa*, leaf shedding and plant death occurred before Day 8 in the 50 PSU salinity treatment. For all three species, Ψ_{md} was significantly lower than Ψ_{pd} for all measured dates (*L. racemosa t*-test BF = 679, *R. mangle t*-test BF = 176 and *A. germinans t*-test BF = 2624; Figure S2 available as Supplementary Data at *Tree Physiology* Online). In *L. racemosa* and *R. mangle* there were progressive reductions in the Ψ_{pd} and Ψ_{md} in the 30 and 50 PSU treatments, most conspicuously on Days 4 and 8 (Figure S2 available as Supplementary Data at *Tree Physiology* Online). *A. germinans* had lower Ψ_{pd} and Ψ_{md} than the other two species over the course of the experiment (Ψ_{pd} BF = 1.2×10^9; Ψ_{md} BF = 2.82×10^{15}; Figure S2 available as Supplementary Data at *Tree Physiology* Online). In only *R. mangle*, increasing salinity led to reductions in LWC (*R. mangle* BF = 2.96; *A. germinans* BF = 0.30; *L. racemosa* BF = 1.02; Figure S3 available as Supplementary Data at *Tree Physiology* Online). No statistical differences were found within species in LT, LMA or ρ_{leaf} across salinity treatments and dates.

The Ψ_{pdd} shifted from negative to positive values as the plants acclimated to substrate salinity concentration. Before the experimental change in salinity (or Day 0), in all species and treatments, the Ψ_{pdd} was ~−1.0 MPa (i.e., Ψ_{pd} was −1.0 MPa more negative than Ψ_{sub}), as expected given night-time transpiration. This level of Ψ_{pdd} was maintained in the 1 and 10 PSU salinity treatment during the duration of the experiment, except in *A. germinans*, which had a much lower Ψ_{pdd} than the other two species. However, on Day 2, for individuals of the three species in the 30 and 50 PSU treatments, Ψ_{pdd} shifted to positive values (i.e., Ψ_{sub} was more negative than Ψ_{pd}), ranging

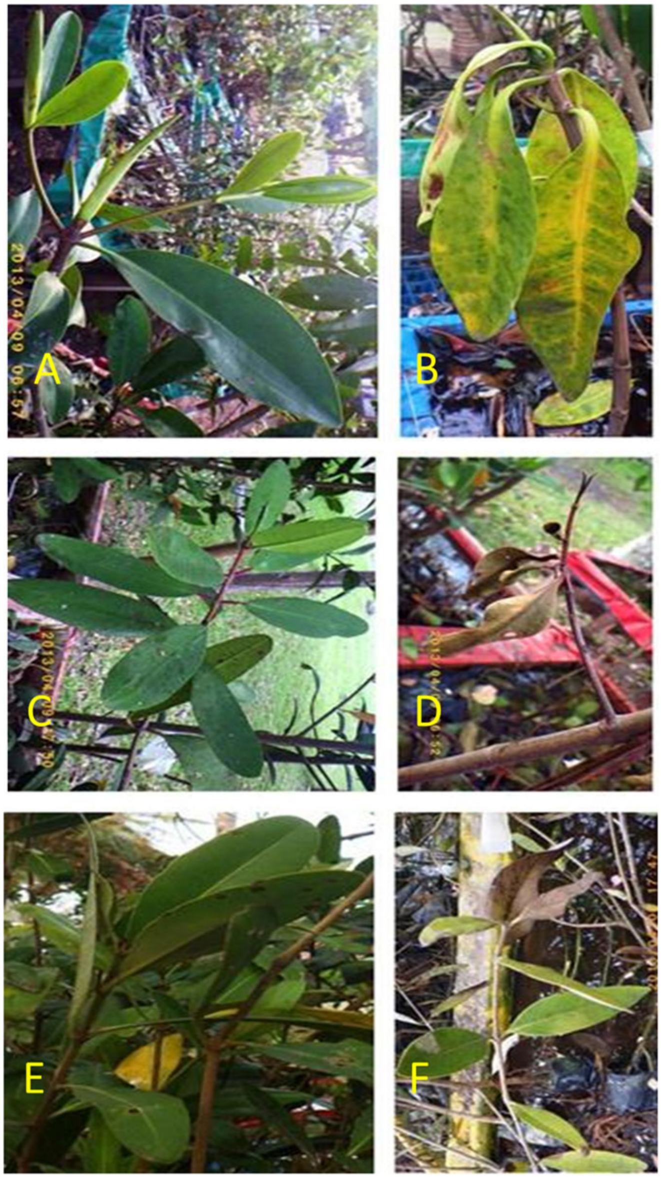

Figure 1. Salinity-induced changes in leaf turgor in saplings of three mangrove species growing in a common garden under understory conditions in the Centro de Investigaciones Costeras La Mancha, Veracruz, México. Photographs correspond to Day 8 for treatments 1 and 50 PSU NaCl. (A) *Rhizophora mangle* 1 PSU, (B) *R. mangle* 50 PSU, (C) *L. racemosa* 1 PSU, (D) *L. racemosa* 50 PSU, (E) *A. germinans* 1 PSU and (F) *A. germinans* 50 PSU. Variations in leaf coloration may have been caused by low light conditions.

between (positive) 2 MPa (in *A. germinans*) to 3 and 4 MPa (in *R. mangle* and *L. racemosa*), probably because the roots had isolated themselves osmotically from the substrate. By Days 4 and 8, Ψ_{pdd} had declined to close to zero ($\Psi_{pd} = \Psi_{sub}$) for *R. mangle* and *L. racemosa*, and for individuals of *A. germinans* in the 50 PSU treatment, Ψ_{pdd} declined to −2.0 MPa by Day 8 (Figure 2). Thus, in our study species, a negative Ψ_{pdd} denoted plant acclimation to substrate salinity.

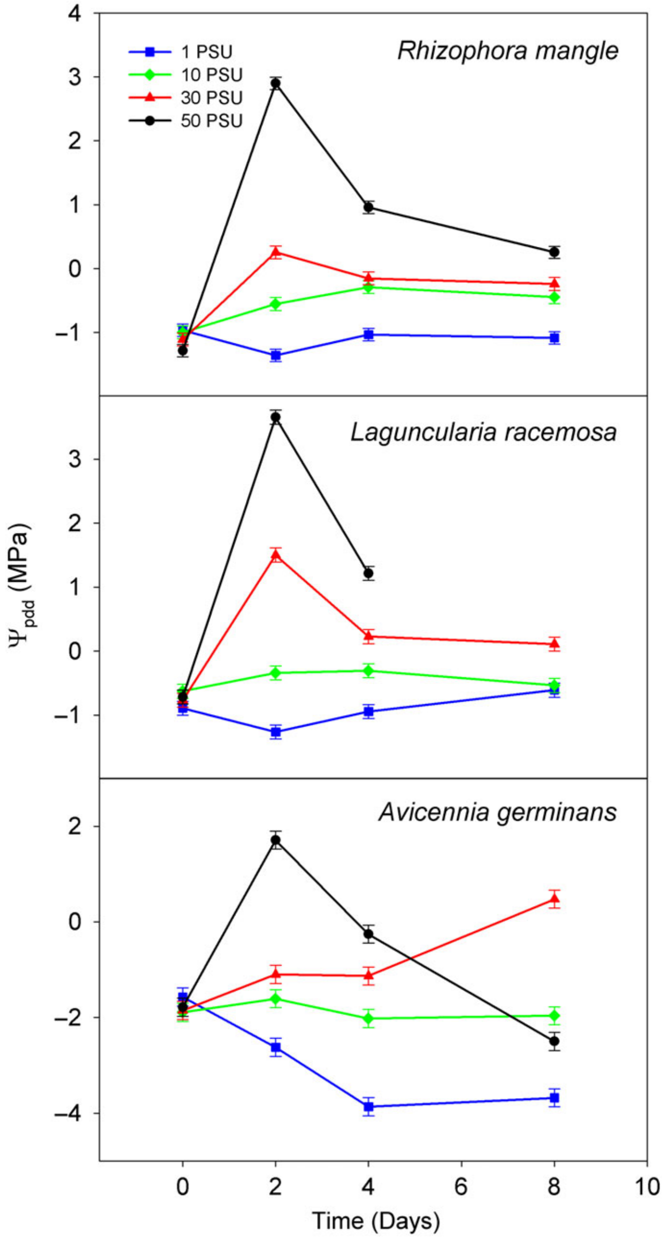

Figure 2. Trajectories of predawn disequilibrium (calculated as the difference between predawn leaf water potential and substrate water potential; $\Psi_{pdd} = \Psi_{pd} - \Psi_{sub}$) for saplings of three mangrove species growing in a common garden and exposed to four salinities in the Centro de Investigaciones Costeras La Mancha, Veracruz, México. *Laguncularia racemosa* individuals in the 50 PSU treatment shed their leaves before Day 8. Osmolality measurements (osm, mmol kg^{-1}) were transformed to MPa, as $\Psi_{sub} = (-0.0026 \times \text{osm}) + 0.024$.

The Ψ_s became progressively more negative with salinity exposure in all three species, which was also reflected in lower values of Ψ_{md} (Figure 3). Two days after the increase in salinity, the Ψ_s in the 50 PSU treatment declined significantly for *L. racemosa* and *R. mangle*, and for *A. germinans* by Day 4, by which time the Ψ_s of *L. racemosa* in the 50 PSU treatment had declined to nearly −4.0 MPa, and a few days afterward, these plants shed their leaves (Figure 3). In contrast, by Days 8 and 33, there

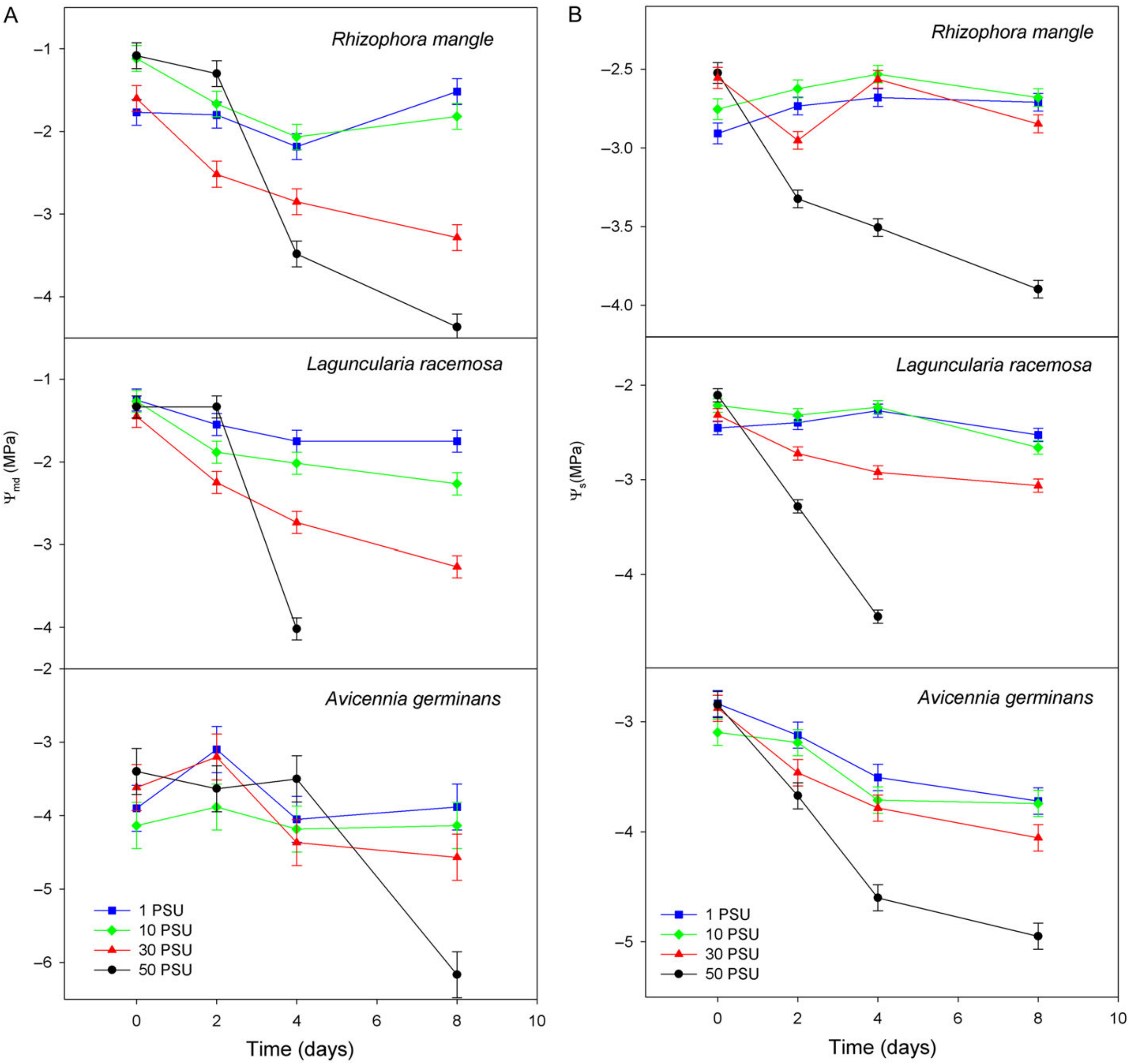

Figure 3. Trajectories of midday leaf water potential (Ψ_{md}, A) and osmotic potential (Ψ_{s}, B) following NaCl addition in saplings of three mangrove species growing in a common garden and exposed to four salinity treatments (1, 10, 30 and 50 PSU) in the Centro de Investigaciones Costeras La Mancha, Veracruz, México. *Laguncularia racemosa* individuals in the 50 PSU treatment shed their leaves before Day 8.

were no significant differences in the Ψ_{s} between the 1 and 10 PSU treatments in the three species, and for *A. germinans* and *R. mangle*, the 30 PSU treatments had intermediate values of Ψ_{s} (mean ± SE = −5.2 ± 0.23 and −3.1 ± 0.05 MPa for *A. germinans* and *R. mangle,* respectively) and the 50 PSU treatments had the lowest values of Ψ_{s} (−6.2 ± 0.15 and −3.4 ± 0.15 MPa). For *L. racemosa*, individuals in the 30 PSU treatment had significantly lower values of Ψ_{s} in comparison with the 1 and 10 PSU treatments (−3.8 ± 0.11 vs −2.4 ± 0.18 and −2.5 ± 0.11 MPa; Figure 3). For all three species, Ψ_{s} is adjusted to the sudden reduction in Ψ_{sub} and consequently there were significant linear relationships among these traits (Figure 4). The slope of the associations between Ψ_{s} and Ψ_{sub} was higher for *L. racemosa* (0.38 ± 0.04), followed by *A. germinans* (0.32 ± 0.05) and *R. mangle* (0.23 ± 0.03) (Figure 4).

For all three species, the g_{s} was significantly reduced by the drastic reduction in Ψ_{sub} in the 30 and 50 PSU treatments throughout the experiment (but no significant reductions were observed for K_{plant}; Figure S4 available as Supplementary Data at *Tree Physiology* Online). For each species, there were significant associations between g_{s} and Ψ_{sub}, and this relationship was stronger in the salt-sensitive *L. racemosa* and weaker

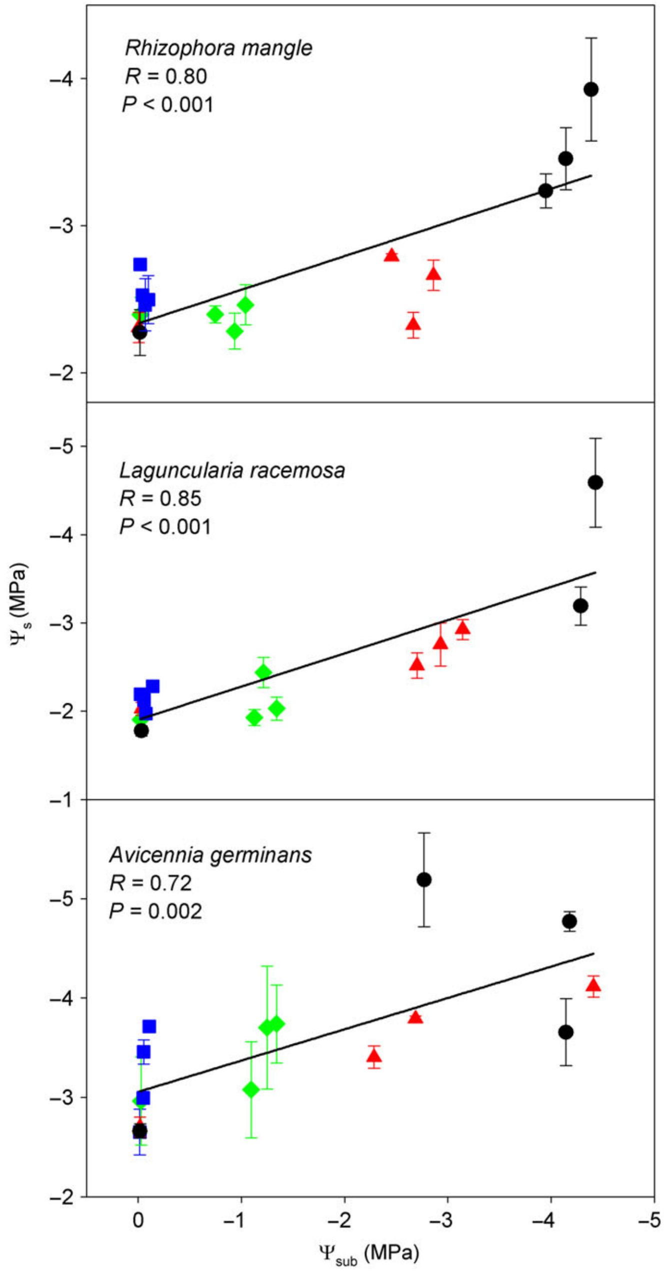

Figure 4. Correlations between leaf osmotic potential (Ψ_s) and substrate water potential (Ψ_{sub}) of saplings of three mangrove species growing in a common garden and exposed to four salinity treatments (treatments (squares = 0 PSU; diamonds = 10 PSU; triangles = 30 PSU; circles = 50 PSU)) in the Centro de Investigaciones Costeras La Mancha, Veracruz, México. *Laguncularia racemosa* individuals in the 50 PSU treatment shed their leaves before Day 8.

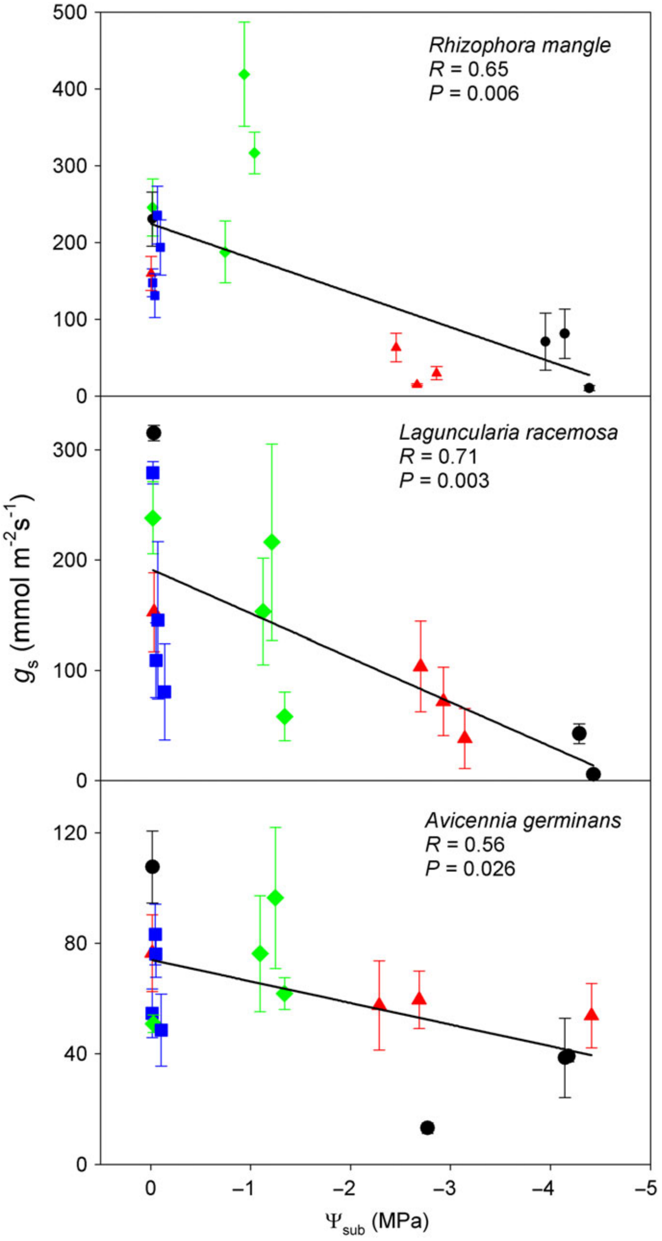

Figure 5. Correlations between stomatal conductance (g_s) and substrate water potential (Ψ_{sub}) of saplings of three mangrove species growing in a common garden and exposed to four salinity treatments (treatments (squares = 0 PSU; diamonds = 10 PSU; triangles = 30 PSU; circles = 50 PSU)) in the Centro de Investigaciones Costeras La Mancha, Veracruz, México. *Laguncularia racemosa* individuals in the 50 PSU treatment shed their leaves before Day 8.

in the salt-tolerant *A. germinans* (Figure 5). Pooling data across species, K_{plant} was positively correlated with Ψ_s ($K_{plant} = 0.74 + (\Psi_o \times 2.22)$, $R = 0.47$, $P < 0.001$; Figure 6).

Discussion

Our results demonstrate that physiological traits associated with acclimation to salinity in the three mangroves species are coordinated and temporarily decoupled from their substrate. In particular, our results point to a whole-plant coordinated response to sudden reductions in Ψ_{sub} by simultaneously modulating Ψ_{pd}, Ψ_{md}, Ψ_s and K_{plant}. In the mangroves, acclimation to salinity shock is not an instantaneous process, but is instead characterized by delayed response, which eventually results in hydraulic equilibrium between Ψ_{sub} and Ψ_{pd} that is associated with simultaneous reductions in Ψ_s and K_{plant}. Our results suggest that disequilibrium between Ψ_{sub} and Ψ_{pd} in halophytes is

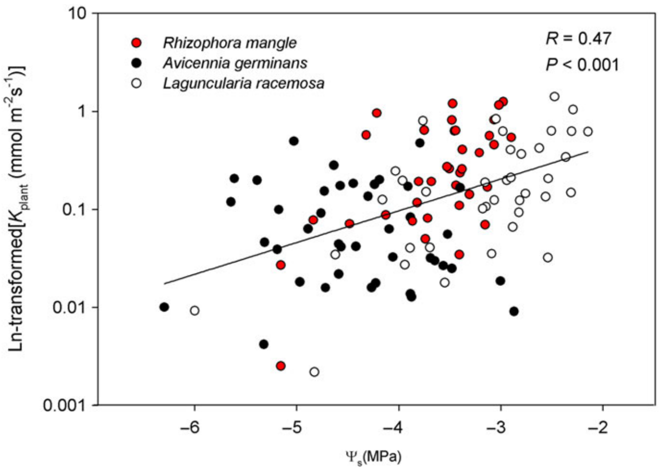

Figure 6. Correlation between whole-plant hydraulic conductance (K_{plant}) and osmotic potential (Ψ_s) of saplings of three mangrove species growing in a common garden and exposed to four salinity treatments (1, 10, 30 and 50 PSU) in the Centro de Investigaciones Costeras La Mancha, Veracruz, México.

not a temporal and unusual process, but a prolonged condition denoting plant acclimation to Ψ_{sub}. Following our time trajectories, we found that the degree of Ψ_{pdd} is dynamic and contingent on substrate water status, as plants actively adjust to a changing salinity environment, which ultimately is reflected in a return to more negative values of Ψ_{pd} after changes in Ψ_{sub}. These results point toward potential diagnostic tools to detect catastrophic salinity stress in mangroves and to understand the linkage between substrate and plant water potentials.

A systemic physiological response to salinity stress: coordination of K_{plant} and g_s with Ψ_s

Previous work has demonstrated that the response of plants to induced drought or salinity stress involves several fast signaling pathways, including the release of nitric oxide, the production of abscisic acid and the activation of Salt Overly Sensitive and High-Affinity K^+ Transporter loci encoding Na^+/H^+ or Na^+/K^+ plasmatic membrane exchangers, all of which could produce systemic responses at the molecular level, and lead to physiological changes including stomatal closure, reduction in elongation rates and Na^+ accumulation in the vacuoles (García-Mata and Lamattina 2001, Davis et al. 2005, Huang et al. 2008, Ji et al. 2013). Our study using physiological metrics demonstrated a systemic response to osmotic stress at the whole-plant scale, involving the coordination of K_{plant} with Ψ_s, and the concomitant reductions in Ψ_{pd} and Ψ_{md}.

Coordination of physiological traits such as photosynthetic rate, leaf structure and wood density has been observed within and across species (Wright et al. 2004, Chave et al. 2009, Reich 2014), providing evidence of concerted mechanisms that plants employ to exploit resources. Our study demonstrates that in mangroves the set of traits that are associated with tolerance to salinity stress are also coordinated, allowing individuals to adjust their physiology and water status to new conditions in a short time scale. In particular, at high salinities, plants reduce g_s and K_{plant} as they experience lower Ψ_{pd} and Ψ_{md}; however, the response to confront acute salinity operates differently across mangrove species. For example, *A. germinans* is a more water-conservative species, with higher tolerance of foliar osmotic loads and the ability to withstand substantially negative soil water potentials; however, this species had lower g_s and therefore lower transpiration rates at optimum conditions than *R. mangle* or *L. racemosa*, probably a by-cost of tolerance of ion toxicity and osmotic stress. Species in the genus *Avicennia* are known to maintain high hydraulic conductance, photosynthetic and transpiration rates, and relative growth at 50–75% seawater salinity, although *A. germinans* had lower photosynthetic rates throughout the experiment than the other two species (Burchett et al. 1984, López-Portillo et al. 2005, Nguyen et al. 2015).

Although mangroves are adapted to fluctuating salinity on a daily or seasonal basis, species-specific limits on the salinity tolerance can cause cellular and metabolic dysfunction. In contrast to *A. germinans*, *L. racemosa* was the least salt-tolerant species in our study. In this species, 30 PSU salinity led to stronger reductions in hydraulic conductivity, g_s and transpiration rates than in the other two species (also see Sobrado 2007). In the 50 PSU treatment, *L. racemosa* was unable to sustain its metabolism. The intrusion of substrate salt within the apoplast (López-Portillo et al. 2014), combined with the potential costs associated with osmotic adjustment and the proportionally strong reduction in carbon acquisition via restriction of g_s and K_{plant}, and/or direct cell death due to ion toxicity (which might have been enhanced by our use of commercial salt), caused osmotic shock or desiccation that may have been critical in causing mangrove mortality in our experimental setting, in a similar fashion as found for other species (Lovelock et al. 2009).

Sensing root water environment: plant responses to changes in Ψ_{sub}

In our study species, as previously reported for other halophytes and drought tolerant species, Ψ_{pd} did not reach equilibrium with Ψ_{sub} even under different Ψ_{sub} treatments (Ourcival et al. 1994, Donovan et al. 2001, 2003). As our experiment was set on hydroponic growing beds, we were able to control substrate heterogeneity, allowing us to simultaneously follow the trajectory of Ψ_{pdd} in three species at different levels of salinity, an approach not previously employed to explore the dynamics of Ψ_{pdd} in halophytes. For our three study species, we found Ψ_{pdd} values up to −1 MPa before the experimental change in salinity, which was consistently maintained in the 1 PSU salinity treatment and, with slight reductions, in the 10 PSU salinity treatment across all measurement dates. In the high salinity treatments (30 and 50 PSU), there were clear changes in Ψ_{sub} that were temporarily decoupled from Ψ_{pd} as the experiment progressed.

The trajectory of Ψ_{pdd} followed three distinguishable stages. (i) A pre-stress stage, during which Ψ_{pdd} was maintained at close to −1 MPa probably due to night-time transpiration and an apoplastic Ψ_s more negative than Ψ_{sub} (Kavanagh et al. 2007, Howard et al. 2009). (ii) An initial shock stage, during which the plants responded to the strongly reduced Ψ_{sub} due to high salinities by drastically reducing g_s, but preserving high Ψ_{pd} and Ψ_{md} values that resulted in positive values of Ψ_{pdd} of up to ~4 MPa. This increase in Ψ_{pdd} is consistent with aquaporin gating at the root symplast, causing momentary hydraulic isolation and reducing root hydraulic conductivities and consequently g_s and K_{plant} (Tan et al. 2013, Vandeleur et al. 2014). Finally, in (iii) there was an asymptotic recovery of Ψ_{pdd}, in which Ψ_{pd} and Ψ_{md} declined and plant water potentials acclimated to the new osmotic conditions of the substrata via foliar osmotic adjustment, although whole-plant hydraulic conductance did not recover toward pre-stress values. The asymptotic recovery phase of predawn disequilibrium included a progressive reduction in Ψ_{pd}, K_{plant} and Ψ_s, probably to avoid the risk of hydraulic failure and reductions in the functionality of root aquaporins.

According to our results and due to the fact that mangrove roots can ultra-filter ions via the suberized and lignified apoplastic barriers (Casparian bands and biseriate exodermis), which account for ~90% of solute exclusion from the transpiration stream (Scholander 1968, Khrisnamurthy et al. 2014), a constant disequilibrium between Ψ_{pd} and Ψ_{sub} may be typical for mangroves. In other words, negative values for Ψ_{pdd} may indicate plant acclimation to substrate salinity. Apoplastic barriers may also channel water toward selected sites in the membrane, which may have a higher density of aquaporins; however, after the addition of salt, especially in the 30 and 50 PSU treatments, a closure of aquaporin channels may occur due to the sudden imbalance in the substrate Na^+/H^+ ratio (Polle and Chen 2015). During this stage, leaf osmolyte concentration started to increase, probably as a response to the increase in Na^+ concentration in the apoplast sap due to non-perfect ultra-filtration of ions (López-Portillo et al. 2014) and sequestration of Na^+ and K^+ in the symplast. In *A. germinans* and *L. racemosa*, the processes of osmotic adjustment may have been active, given that no differences in LWC were found across treatments in the two species, and due to the fact that the slopes of the Ψ_s vs Ψ_{sub} association were relatively high. In contrast, *R. mangle* may have been passively adjusting its Ψ_s, given its significantly lower volume of foliar water in the high salinity treatments (lower LWC in the 50 PSU salinity) and its lower slope in the Ψ_s vs Ψ_{sub} relationship (Morgan 1984). Therefore, in mangroves, the magnitude of foliar osmotic adjustments shows a time-lag response to Ψ_{sub}, but these changes are species specific. Under extreme salinity, when osmotic regulation cannot achieve more negative Ψ_{pd} and Ψ_{md} values than Ψ_{sub}, plant death occurs, as occurred in the 50 PSU salinity treatment of *L. racemosa*.

Given that mangroves are normally subject to cyclic changes in salinity due to tidal influences and coastal dynamics, plants may recover their original values of g_s and K_{plant} following new inputs of fresh water (Ball and Farquhar 1984*a*). However, if salinity above the normal conditions in which the plants have grown is maintained for longer periods, even the most salinity-tolerant plants may not be able to cope with the interactive effects of ion toxicity and the metabolic restrictions of a low carbon acquisition, especially for understory seedlings and saplings, may not be able to recover their gas exchange functions and thus, may die. Further studies should explore the role of aquaporin gating under changes in Ψ_{pdd} that may cause hydraulic isolation, and the mechanisms that determine the elicitation of cascades of signaling events aiming to reduce plant water potentials and reducing overall hydraulic conductivity.

Supplementary Data

Supplementary data for this article are available at *Tree Physiology* Online.

Acknowledgments

We acknowledge Mr Enrique Barradas and the personal of CICOLMA-La Mancha, INECOL for the use of facilities, and Dr Raul Canino (UABC), MSc Ariadna Martínez, Daniela Cela, and MSc Sandra Rocha (INECOL) for the chemical analyses of salt. We appreciate the comments of K. Krauss and one anonymous reviewer to improve a previous version of this paper.

Conflict of interest

None declared.

Funding

R.M-A. gratefully acknowledges the support by UC-MEXUS-CONACYT postdoctoral program and UC-MEXUS small grants program, and current support by CICESE-B0F081-681-117. C.M. acknowledges support from CONACYT (Doctoral scholarship 33762) and the Programa de Posgrado en Ciencias Biológicas, UNAM. J.L.P. acknowledges support from the Texas A & M University and Consejo Nacional de Ciencia y Tecnología (CONACYT) Collaborative Research Grant Program and INECOL contract #20011/10016.

References

Ball MC (1988) Ecophysiology of mangroves. Trees Struct Funct 2:129–142.

Ball MC (2002) Interactive effects of salinity and irradiance on growth: implications for mangrove forest structure along salinity gradients. Trees Struct Funct 16:126–139.

Ball MC, Farquhar GD (1984*a*) Photosynthetic and stomatal responses of the grey mangrove, *Avicennia marina*, to transient salinity conditions. Plant Physiol 74:7–11.

Ball MC, Farquhar GD (1984*b*) Photosynthetic and stomatal responses of two mangrove species, *Aegiceras corniculatum* and *Avicennia marina*, to long term salinity and humidity conditions. Plant Physiol 74:1–6.

Bartlett MK, Scoffoni C, Ardy R, Zhang Y, Sun S, Cao KF, Sack L (2012) Rapid determination of comparative drought tolerance traits: using an osmometer to predict turgor loss point. Methods Ecol Evol 3:880–888.

Buck AL (1981) New equations for computing vapor-pressure and enhancement factor. J Appl Meteorol 20:1527–1532.

Burchett MD, Field CD, Pulkownik A (1984) Salinity, growth and root respiration in the grey mangrove, *Avicennia marina*. Physiol Plant 60:113–118.

Chave J, Coomes D, Jansen S, Lewis SL, Swenson NG, Zanne AE (2009) Towards a worldwide wood economics spectrum. Ecol Lett 12:351–366.

Davis WJ, Kudoyarova G, Hartung W (2005) Long-distance ABA signaling and its relation to other signaling pathways in the detection of soil drying and the mediation of the plant response to drought. J Plant Growth Regul 24:285–295.

Donovan LA, Grisé DJ, West JB, Pappert RA, Alder NN, Richards JH (1999) Predawn disequilibrium between plant and soil water potentials in two cold-desert shrubs. Oecologia 120:209–217.

Donovan LA, Linton MJ, Richards JH (2001) Predawn plant water potential does not necessarily equilibrate with soil water potential under well-watered conditions. Oecologia 129:328–335.

Donovan LA, Richards JH, Linton MJ (2003) Magnitude and mechanisms of disequilibrium between predawn plant and soil water potentials. Ecology 84:463–470.

Ewers FW, Lopez-Portillo J, Angeles G, Fisher JB (2004) Hydraulic conductivity and embolism in the mangrove tree *Laguncularia racemosa*. Tree Physiol 24:1057–1062.

García-Mata C, Lamattina L (2001) Nitric oxide induces stomatal closure and enhances the adaptive plant responses against drought stress. Plant Physiol 126:1196–1204.

Guyot G, Scoffoni C, Sack L (2012) Combined impacts of irradiance and dehydration on leaf hydraulic conductance: insights into vulnerability and stomatal control. Plant Cell Environ 35:857–871.

Howard AR, Van Iersel MW, Richards JH, Donovan LA (2009) Night-time transpiration can decrease hydraulic redistribution. Plant Cell Environ 32:1060–1070.

Huang S, Spielmeyer W, Lagudah ES, Munns R (2008) Comparative mapping of HKT genes in wheat, barley, and rice, key determinants of Na^+ transport and salt tolerance. J Exp Bot 59:927–937.

James JJ, Alder NN, Mühling KH, Läuchli AE, Shackel KA, Donovan LA, Richards JH (2006) High apoplastic solute concentrations in leaves alter water relations of the halophytic shrub, *Sarcobatus vermiculatus*. J Exp Bot 57:139–147.

Jarosz AF, Wiley J (2014) What are the odds? A practical guide to computing and reporting Bayes factors. J Probl Solving 7:2–9.

Ji H, Pardo JM, Batellic G, Van Oostend MJ, Bressane RA, Li X (2013) The salt overly sensitive (SOS) pathway: established and emerging roles. Mol Plant 6:275–286.

Kavanagh KL, Pangle R, Schotzko AD (2007) Nocturnal transpiration causing disequilibrium between soil and stem predawn water potential in mixed conifer forests of Idaho. Tree Physiol 27:621–629.

Krauss KW, Allen JA (2003) Influences of salinity and shade on seedling photosynthesis and growth of two mangrove species, *Rhizophora mangle* and *Bruguiera sexangula*, introduced to Hawaii. Aquat Bot 77:311–324.

Krauss KW, Ball MC (2013) On the halophytic nature of mangroves. Trees Struct Funct 27:7–11.

Krishnamurthy P, Jyothi-Prakash PA, Qin L, He J, Lin Q, Loh CS, Kumar PP (2014) Role of root hydrophobic barriers in salt exclusion of a mangrove plant *Avicennia officinalis*. Plant Cell Environ 37: 1656–1671.

López-Hoffman L, DeNoyer JL, Monroe IE, Shaftel R, Anten NP, Martínez-Ramos M, Ackerly DD (2006) Mangrove seedling net photosynthesis, growth, and survivorship are interactively affected by salinity and light. Biotropica 38:606–616.

López-Hoffman L, Anten NP, Martinez-Ramos M, Ackerly DD (2007) Salinity and light interactively affect neotropical mangrove seedlings at the leaf and whole plant levels. Oecologia 150:545–556.

López-Portillo J, Ewers FW, Angeles G (2005) Sap salinity effects on xylem conductivity in two mangrove species. Plant Cell Environ 28:1285–1292.

López-Portillo J, Ewers FW, Méndez-Alonzo R, Paredes López C, Angeles G, Alarcón Jiménez AL, Lara-Domínguez AL, Torres Barrera MC (2014) Dynamic control of osmolality and ionic composition of the xylem sap in two mangrove species. Am J Bot 10:1013–1022.

Lovelock CE, Ball MC, Feller IC, Engelbrecht BM, Ling Ewe M (2006) Variation in hydraulic conductivity of mangroves: influence of species, salinity, and nitrogen and phosphorus availability. Physiol Plant 127:457–464.

Lovelock CE, Ball MC, Martin KC, Feller IC (2009) Nutrient enrichment increases mortality of mangroves. PLoS One 4:e5600.

Lovelock CE, Krauss KW, Osland MJ, Reef R, Ball MC (2016) The physiology of mangrove trees with changing climate. In: Goldstein G, Santiago LS (eds) Tropical tree physiology. Springer, New York, pp 149–179.

Lugo AE, Snedaker SC (1974) The ecology of mangroves. Annu Rev Ecol Syst 5:39–64.

Melcher PJ, Goldstein G, Meinzer FC, Yount DE, Jones TJ, Holbrook NM, Huang CX (2001) Water relations of coastal and estuarine *Rhizophora mangle*: xylem pressure potential and dynamics of embolism formation and repair. Oecologia 126:182–192.

Moray C, Hua X, Bromham L (2015) Salt tolerance is evolutionarily labile in a diverse set of angiosperm families. BMC Evol Biol 15:1–10.

Morgan JM (1984) Osmoregulation and water stress in higher plants. Annu Rev Plant Physiol 35:299–319.

Nardini A, Salleo S (2000) Limitation of stomatal conductance by hydraulic traits: sensing or preventing xylem cavitation? Trees Struct Funct 15:14–24.

Naidoo G (1987) Effects of salinity and nitrogen on growth and water relations in the mangrove, *Avicennia marina* (Forsk.) Vierh. New Phytol 107:317–325.

Nguyen HT, Stanton DE, Schmitz N, Farquhar GD, Ball MC (2015) Growth responses of the mangrove *Avicennia marina* to salinity: development and function of shoot hydraulic systems require saline conditions. Ann Bot-London 115:397–407.

Ourcival JM, Berger A (1995) Equilibrium between soil water potential and predawn water potential of two pre-Saharan shrub species of Tunisia. J Arid Environ 30:175–183.

Ourcival JM, Floret C, Le Floch E, Pontanier R (1994) Water relations between two perennial species in the steppes of southern Tunisia. J Arid Environ 28:333–350.

Parida AK, Jha B (2010) Salt tolerance mechanisms in mangroves: a review. Trees Struct Funct 24:199–217.

Patel NT, Gupta A, Pandey AN (2010) Strong positive growth responses to salinity by *Ceriops tagal*, a commonly occurring mangrove of the Gujarat coast of India. AoB Plants 2010:plq011, 10.1093/aobpla/plq011.

Pérez-Harguindeguy N, Díaz S, Garnier E et al. (2013) New handbook for standardised measurement of plant functional traits worldwide. Aust J Bot 61:167–234.

Pilsen MEQ (1998) An introduction to the chemistry of the sea. Prentice Hall, New York.

Polle A, Chen S (2015) On the salty side of life: molecular, physiological and anatomical adaptation and acclimation of trees to extreme habitats. Plant Cell Environ 38:1794–1816.

R Development Core Team (2016) R: a language and environment for statistical computing. R Foundation for Statistical Computing, Vienna, Austria. https://www.R-project.org

Reef R, Lovelock CE (2015) Regulation of water balance in mangroves. Ann Bot-London 115:385–395.

Reich PB (2014) The world-wide 'fast–slow' plant economics spectrum: a traits manifesto. J Ecol 102:275–301.

Robert EM, Koedam N, Beeckman H, Schmitz N (2009) A safe hydraulic architecture as wood anatomical explanation for the difference in distribution of the mangroves *Avicennia* and *Rhizophora*. Funct Ecol 23:649–657.

Scholander PF (1968) How mangroves desalinate seawater. Physiol Plant 21:251–261.

Shi S, Huang Y, Zeng K, Tan F, He H, Huang J, Fu Y (2005) Molecular phylogenetic analysis of mangroves: independent evolutionary origins of vivipary and salt secretion. Mol Phylogenet Evol 34:159–166.

Sobrado MA (2007) Relationship of water transport to anatomical features in the mangrove *Laguncularia racemosa* grown under contrasting salinities. New Phytol 173:584–591.

Suárez N, Medina E (2005) Salinity effect on plant growth and leaf demography of the mangrove, *Avicennia germinans* L. Trees Struct Funct 19:728–734.

Suárez N, Medina E (2006) Influence of salinity on Na^+ and K^+ accumulation, and gas exchange in *Avicennia germinans*. Photosynthetica 44:268–274.

Suárez N, Sobrado MA (2000) Adjustment in leaf water relations of mangrove (*Avicennia germinans*) seedlings grown in a salinity gradient. Tree Physiol 20:277–282.

Suárez N, Sobrado MA, Medina E (1998) Salinity effects on the leaf water relations components and ion accumulation patterns in *Avicennia germinans* (L.) seedlings. Oecologia 114:299–304.

Tan WK, Lin Q, Lim TM, Kumar P, Loh CS (2013) Dynamic secretion changes in the salt glands of the mangrove tree species *Avicennia officinalis* in response to a changing saline environment. Plant Cell Environ 36:1410–1422.

Vandeleur RK, Sullivan W, Athman A, Jordans C, Gilliham M, Kaiser BN, Tyerman SD (2014) Rapid shoot-to-root signalling regulates root hydraulic conductance via aquaporins. Plant Cell Environ 37: 520–538.

Wang W, Yan Z, You S, Zhang Y, Chen L, Lin G (2011) Mangroves: obligate or facultative halophytes? A review. Trees Struct Funct 25: 953–963.

Wright IJ, Reich PB, Westoby M et al. (2004) The worldwide leaf economics spectrum. Nature 428:821–827.

Yan Z, Wang W, Tang D (2007) Effect of different time of salt stress on growth and some physiological processes of *Avicennia marina* seedlings. Mar Biol 152:581–587.

Zhu Z, Zhang RF, Liu TW, Zheng HL (2011) Solute accumulation and osmotic adjustment characteristics of the mangrove *Avicennia marina* under NaCl-induced salinity stress. Bot Mar 54:335–341.

Zhu Z, Chen J, Zheng HL (2012) Physiological and proteomic characterization of salt tolerance in a mangrove plant, *Bruguiera gymnorrhiza* (L.) Lam. Tree Physiol 32:1378–1388.